



Brief paper

Globally exponentially stable attitude and gyro bias estimation with application to GNSS/INS integration[☆]



Håvard Fjær Grip^a, Thor I. Fossen^b, Tor A. Johansen^b, Ali Saberi^c

^a Department of Engineering Cybernetics, Norwegian University of Science and Technology (NTNU), 7491 Trondheim, Norway

^b Center for Autonomous Marine Operations and Systems, Department of Engineering Cybernetics, NTNU, 7491 Trondheim, Norway

^c School of Electrical Engineering and Computer Science, Washington State University, Pullman, WA 99164, USA

ARTICLE INFO

Article history:

Received 7 August 2012

Received in revised form

6 July 2014

Accepted 5 September 2014

Available online 17 November 2014

Keywords:

Guidance, navigation, and control of vehicles

Nonlinear observer and filter design

ABSTRACT

This paper deals with the construction of nonlinear observers for navigation purposes. We first present a globally exponentially stable observer for attitude and gyro bias, based on gyro measurements and two or more pairs of vector measurements. We avoid the well-known topological obstructions to global stability by not confining the attitude estimate to $SO(3)$, but rather estimating a full rotation matrix with nine degrees of freedom. We also show how the attitude can be estimated under a relaxed persistency-of-excitation condition, with a single vector measurement as a special case. Next, we use the attitude observer to construct a globally exponentially stable observer for GNSS/INS integration, based on accelerometer, gyro, and magnetometer measurements, as well as GNSS measurements of position and (optionally) velocity. We verify the stability properties of the design using experimental data from a light fixed-wing aircraft.

© 2014 Elsevier Ltd. All rights reserved.

1. Introduction

Navigation is the task of determining an object's position, velocity, or attitude based on various types of information. For decades the Kalman filter, and nonlinear extensions thereof, have been used to provide integrated navigation solutions based on different types of measurements. There is nevertheless a current interest in the design of nonlinear navigation observers, which can provide explicit stability guarantees and reduced computational complexity.

Attitude is typically estimated by comparing a set of vectors measured in the body-fixed coordinate frame with a set of reference vectors in a reference frame. The attitude can be algebraically resolved using two or more pairs of non-parallel vectors (see

Shuster & Oh, 1981), but it is beneficial to integrate vector measurements with gyro measurements to improve the estimator bandwidth and to mitigate the effect of noise. An overview of early attitude estimators based on the extended Kalman filter (EKF) is provided by Lefferts, Markley, and Shuster (1982). Crassidis, Markley, and Cheng (2007) survey more recent results using the EKF as well as other estimation techniques. In the domain of nonlinear attitude observers with stability guarantees, the work of Salcudean (1991) is important, and it has been built upon by Thienel and Sanner (2003) and Vik and Fossen (2001). The observers based on Salcudean's work assume that the attitude is available as an explicit measurement. Observers that make direct use of vector measurements have been presented by Mahony, Hamel, and Pflimlin (2008), Hamel and Mahony (2006) and Vasconcelos, Silvestre, and Oliveira (2008).

Attitude can be represented by Euler angles, but more commonly a unit quaternion or a rotation matrix is used. For a continuous observer with estimates on the unit sphere or $SO(3)$, topological obstructions prevent global asymptotic stability (see Bhat & Bernstein, 2000). These topological obstructions can be avoided by allowing the attitude estimate to evolve on a larger state space; this strategy has recently been employed by Batista, Silvestre, and Oliveira (2011a,b, 2012b) and by the authors (Grip, Saberi, & Johansen, 2011, 2012b), by estimating a matrix with nine degrees of freedom that converges to a rotation matrix on $SO(3)$.

[☆] The work of Håvard Fjær Grip was partially supported by the Research Council of Norway, project no. 197491. The work of Ali Saberi was partially supported by NAVY grants ONR KKK7775B001 and ONR KKK7605B0012. The material in this paper was partially presented at the 2012 American Control Conference (ACC 2012), June 27–29, 2012, Montréal, Canada. This paper was recommended for publication in revised form by Associate Editor Warren E. Dixon under the direction of Editor Andrew R. Teel.

E-mail addresses: grip@itk.ntnu.no (H.F. Grip), fossen@ieee.org (T.I. Fossen), torj@itk.ntnu.no (T.A. Johansen), saberi@eecs.wsu.edu (A. Saberi).

<http://dx.doi.org/10.1016/j.automatica.2014.10.076>
0005-1098/© 2014 Elsevier Ltd. All rights reserved.

Batista et al. (2012b) and Batista, Silvestre, and Oliveira (2012c) also considered the use of a separate observer to produce globally exponentially stable gyro bias estimates, although their approach requires stationary reference vectors. Attitude estimation using a single vector measurement has been considered by several authors (Batista et al., 2011b; Batista, Silvestre, & Oliveira, 2012a; Kinsey & Whitcomb, 2007; Lee, Leok, McClamroch, & Sanyal, 2007; Mahony, Hamel, Trumpf, & Lageman, 2009) and is possible under a persistency-of-excitation (PE) condition.

In many applications, a combination of inertial instruments and a satellite navigation system is available, often together with additional sensors such as altimeters and magnetometers. The integration of satellite and inertial measurements, referred to as GNSS/INS integration, has been studied for several decades (Maybeck, 1979; Phillips & Schmidt, 1996), typically based on the EKF. Vik and Fossen (2001) designed a nonlinear GNSS/INS integration observer with exponential stability results, based on the assumption that an independent attitude measurement was available. When an independent attitude measurement is not available, one may look for vector measurements that can be used for attitude estimation. The accelerometer offers one such measurement, but the corresponding reference vector (the sum of the gravity vector and the vehicle acceleration in the reference frame) is not explicitly available. Hua (2010) exploited the implicit availability of this reference vector in the derivatives of the GNSS measurements, by making use of GPS velocity information in combination with inertial measurements and a magnetometer.

1.1. Contributions of this paper

In this paper we begin by considering the attitude estimation problem based on gyro and vector measurements. We employ the same strategy as Batista et al. (2011a,b, 2012b) and Grip et al. (2011, 2012b) of letting the attitude be estimated as a full 3×3 matrix, the main contribution being the additional estimation of gyro bias. The bias estimation is of lower order than that of Batista et al. (2012b,c) and is capable of handling time-varying reference vectors, which is a prerequisite in the latter part of our paper. We nominally assume availability of at least two pairs of non-parallel vectors; however, as a fault-tolerance strategy we prove that the observer can be employed without gyro bias estimation using a single vector pair, under a persistency-of-excitation (PE) condition.

We continue by constructing a GNSS/INS integration observer based on the newly developed attitude observer. To do so, we leverage a general design framework for cascaded nonlinear and linear systems previously presented by Grip et al. (2012b), where a simplified version of the observer, without gyro bias estimation, was used as an application example. The design framework provides flexibility in handling different GNSS measurement setups, including partial or no velocity information. We prove global exponential stability of the observer error, and verify the stability results using an experimental platform consisting of a GNSS receiver and an inertial measurement unit (IMU) mounted in a light fixed-wing aircraft. A preliminary version of this paper was presented at the 2012 American Control Conference (Grip, Fossen, Johansen, & Saberi, 2012a).

1.2. Notation and preliminaries

For a vector or matrix X , X' denotes its transpose. The operator $\|\cdot\|$ denotes the Euclidean norm for vectors and the Frobenius norm for matrices. For a symmetric positive-semidefinite matrix X , the minimum eigenvalue is denoted by $\lambda_{\min}(X)$. The skew-symmetric part of a square matrix X is denoted by $\mathbb{P}_a(X) = \frac{1}{2}(X - X')$. For a vector $x \in \mathbb{R}^3$, $S(x)$ denotes the skew-symmetric matrix such that for any $y \in \mathbb{R}^3$, $S(x)y = x \times y$. The linear function $\text{vex}(X)$ such

that $S(\text{vex}(X)) = X$ and $\text{vex}(S(x)) = x$ is well-defined for all 3×3 skew-symmetric matrix arguments. The function $\text{sat}_l(\cdot)$ denotes a component-wise saturation of its vector or matrix argument to the interval $[-L, L]$.

When referring to the notion of *global exponential stability*, we apply the definition of Michel, Hou, and Liu (2008), specialized to our circumstances. In particular, for the *motion* $x(t)$, originating from an initial condition $x(0)$ at time $t = 0$, the origin is globally exponentially stable (or exponentially stable in the large) if there exist an $\alpha > 0$, $\gamma > 0$, and for each $\beta > 0$, there exists a $k(\beta) > 0$ such that $\|x(t)\| \leq k(\beta)\|x(0)\|^\gamma e^{-\alpha t}$, whenever $\|x(0)\| < \beta$.

2. Attitude estimation

We operate with a body-fixed frame (BODY), indicated by the superscript ^b, and an inertial coordinate frame. For the sake of continuity with later sections, we make the simplifying assumption that the inertial coordinate frame is the local North-East-Down (NED) coordinate frame and use the superscript ⁿ. The attitude is represented by $R \in \text{SO}(3)$, which rotates any vector w^b from BODY to NED according to the relationship $w^n = R w^b$. The kinematics of the rotation matrix satisfies

$$\dot{R} = RS(\omega^b), \quad (1)$$

where ω^b is the angular velocity of the BODY frame relative to the NED frame, decomposed in BODY coordinates.

We assume availability of a gyro measurement $\omega_m^b = \omega^b + b$, where b is an unknown gyro bias. We furthermore assume availability of k body-fixed vector measurements w_1^b, \dots, w_k^b , as well as corresponding reference vectors $w_1^n, \dots, w_k^n = R w_1^b, \dots, R w_k^b$, which are allowed to be time-varying.

Assumption 1. There exists a $c_{\text{obs}} > 0$ such that, for each $t \geq 0$, there are $i, j \in 1, \dots, k$ such that $\|w_i^n \times w_j^n\| \geq c_{\text{obs}}$.

Assumption 2. The gyro bias b is constant, and there exists a known constant $M_b > 0$ such that $\|b\| \leq M_b$.

We also make the physically reasonable assumption that ω^b and w_1^n, \dots, w_k^n are continuous in t and uniformly bounded.

2.1. Observer

We introduce an observer for R and b given by

$$\dot{\hat{R}} = \hat{R}S(\omega_m^b - \hat{b}) + \sigma K_P J(t, \hat{R}), \quad (2a)$$

$$\dot{\hat{b}} = \text{Proj}(\hat{b}, -k_l \text{vex}(\mathbb{P}_a(\hat{R}'_s K_P J(t, \hat{R})))), \quad (2b)$$

where K_P is a symmetric positive-definite gain matrix, $k_l > 0$ is a scalar gain, $\sigma \geq 1$ is a scaling factor that will be tuned to achieve stability, and $\hat{R}_s = \text{sat}_1(\hat{R})$. The function $\text{Proj}(\cdot, \cdot)$ represents a parameter projection (see Appendix), which ensures that $\|\hat{b}\|$ remains smaller than some design constant $M_{\hat{b}} > M_b$. The function $J(t, \hat{R})$ is a stabilizing injection term on the form

$$J(t, \hat{R}) = \sum_{j=1}^q (A_j^n(t) - \hat{R}A_j^b(t))A_j^b(t)', \quad (3)$$

where the time-varying matrices $A_j^n(t) \in \mathbb{R}^{3 \times r_j}$ and $A_j^b(t) \in \mathbb{R}^{3 \times r_j}$, $j = 1, \dots, q$, satisfy the following property.

Property 1. For each $j \in 1, \dots, q$, the matrices $A_j^n(t)$ and $A_j^b(t)$ are piecewise continuous in t and uniformly bounded by $\|A_j^n(t)\| = \|A_j^b(t)\| \leq M_A$. Furthermore, they satisfy the relationship $A_j^n(t) = R A_j^b(t)$, and there exists a constant $\varepsilon > 0$ such that for all $t \geq 0$, $Q^n(t) := \sum_{j=1}^q A_j^n(t)A_j^n(t)' \geq \varepsilon I_3$.

It follows directly from [Property 1](#) that

$$J(t, \hat{R}) = (R - \hat{R})Q^b(t), \quad (4)$$

where $Q^b(t) := \sum_{j=1}^q A_j^b(t)A_j^b(t)' = R'Q^n(t)R \geq \varepsilon I_3$. In the following, we shall mostly refer to J , A_j^b , A_j^n , Q^b , and Q^n without function arguments.

The matrices A_j^n and A_j^b can be constructed in several ways to satisfy [Property 1](#). With two vector measurements, the choice

$$A_1^t = \begin{bmatrix} \frac{w_1^t}{\|w_1^t\|} & \frac{S(w_1^t)w_2^t}{\|S(w_1^t)w_2^t\|} & \frac{S^2(w_1^t)w_2^t}{\|S^2(w_1^t)w_2^t\|} \end{bmatrix}, \quad (5)$$

where $\iota \in \{n, b\}$, yields orthogonal matrices satisfying $A_1^n A_1^{b'} = R$, which corresponds to the algebraic TRIAD solution ([Shuster & Oh, 1981](#)). Inspired by the TRIAD algorithm, the authors have previously used the matrices ([Grip et al., 2011, 2012b](#))

$$A_1^t = [w_1^t \quad S(w_1^t)w_2^t \quad S^2(w_1^t)w_2^t]. \quad (6)$$

An even simpler choice is

$$A_1^t = [w_1^t \quad w_2^t \quad S(w_1^t)w_2^t]. \quad (7)$$

With this choice the injection term is closely related to that of [Batista et al. \(2011a\)](#).

2.2. Stability

Defining the estimation errors $\tilde{R} = R - \hat{R}$ and $\tilde{b} = b - \hat{b}$, we obtain the error dynamics

$$\dot{\tilde{R}} = R S(\omega^b) - \hat{R} S(\omega_m^b - \hat{b}) - \sigma K_P J, \quad (8a)$$

$$\dot{\tilde{b}} = -\text{Proj}(\hat{b}, -k_l \text{vex}(\mathbb{P}_a(\hat{R}_s' K_P J))). \quad (8b)$$

Lemma 1. Suppose that [Assumptions 1](#) and [2](#) hold and that A_j^b and A_j^n , $j = 1, \dots, q$, have been designed to satisfy [Property 1](#). For any given choice of K_P and k_l , there exists a $\sigma^* \geq 1$ such for all $\sigma \geq \sigma^*$, the origin of the error dynamics (8) is exponentially stable, and all initial conditions satisfying $\|\tilde{b}(0)\| \leq M_b$ are contained in the region of attraction.

Proof. We can rewrite the error dynamics as

$$\dot{\tilde{R}} = \tilde{R} S(\omega^b + \tilde{b}) - R S(\tilde{b}) - \sigma K_P J, \quad (9a)$$

$$\dot{\tilde{b}} = -\text{Proj}(\hat{b}, -k_l \text{vex}(\mathbb{P}_a(\hat{R}_s' K_P J))). \quad (9b)$$

Defining the function $P = \frac{1}{2} \|\tilde{b}\|^2$, the derivative along the trajectories of the system is $\dot{P} = \hat{b}' \text{Proj}(\hat{b}, -k_l \text{vex}(\mathbb{P}_a(\hat{R}_s' K_P J)))$, for which we have that $\|\tilde{b}\| \geq M_b \implies \dot{P} \leq 0$ (see [Grip et al., 2012a](#), Lemma 3). Hence, $\|\tilde{b}\|$ cannot escape the region $\|\tilde{b}\| \leq M_b$ for any solution of the system. We shall study the trajectories of the function

$$V(t, \tilde{R}, \tilde{b}) = \frac{1}{2} \|\tilde{R}\|^2 - \ell \text{tr}(S(\tilde{b})\tilde{R}'\tilde{R}) + \frac{\ell\sigma}{k_l} \|\tilde{b}\|^2,$$

where $0 < \ell \leq 1$ is yet to be determined, using the knowledge that $\|\tilde{b}\| \leq M_b$, which implies $\|\tilde{b}\| \leq M_b := M_b + M_b$.

Using the properties that (for arbitrary $X \in \mathbb{R}^{3 \times 3}$ and $x \in \mathbb{R}^3$) $|\text{tr}(X)| \leq \sqrt{3}\|X\|$, $\|RX\| = \|X\|$, and $\|S(x)\| = \sqrt{2}\|x\|$, we have $V \geq \frac{1}{2} \|\tilde{R}\|^2 - \ell\sqrt{6}\|\tilde{b}\|\|\tilde{R}\| + \frac{\ell}{k_l} \|\tilde{b}\|^2$, and hence V is positive definite if $\ell < 1/(3k_l)$. Similarly, $V \leq \frac{1}{2} \|\tilde{R}\|^2 + \ell\sqrt{6}\|\tilde{b}\|\|\tilde{R}\| + \frac{\ell}{k_l} \|\tilde{b}\|^2$, and it follows that there are positive constants α_1 and α_2 such that

$\alpha_1(\|\tilde{R}\|^2 + \|\tilde{b}\|^2) \leq V \leq \alpha_2(\|\tilde{R}\|^2 + \|\tilde{b}\|^2)$. The derivative of V along the trajectories of (9) satisfies

$$\begin{aligned} \dot{V} = & \text{tr}(\tilde{R}'(\tilde{R}S(\omega^b + \tilde{b}) - RS(\tilde{b}))) - \sigma \text{tr}(\tilde{R}'K_P J) \\ & + \ell \text{tr}(S(\text{Proj}(\hat{b}, -k_l \text{vex}(\mathbb{P}_a(\hat{R}_s' K_P J))))\tilde{R}'\tilde{R} \\ & - \ell \text{tr}(S(\tilde{b})S'(\omega^b)R'\tilde{R}) - \ell \text{tr}(S(\tilde{b})R'\tilde{R}S(\omega^b + \tilde{b})) \\ & + \ell \text{tr}(S(\tilde{b})R'RS(\tilde{b})) + \ell\sigma \text{tr}(S(\tilde{b})R'K_P J) \\ & - \frac{2\ell\sigma}{k_l} \tilde{b}' \text{Proj}(\hat{b}, -k_l \text{vex}(\mathbb{P}_a(\hat{R}_s' K_P J))). \end{aligned} \quad (10)$$

We now consider the terms on the right-hand side of Eq. (10), starting with the second term. From Eq. (4) and [Property 1](#),

$$\begin{aligned} \text{tr}(\tilde{R}'K_P J) &= \text{tr}(\tilde{R}'K_P \tilde{R}Q^b) = \text{tr}(K_P \tilde{R}Q^b \tilde{R}') \\ &\geq \lambda_{\min}(K_P) \text{tr}(\tilde{R}Q^b \tilde{R}') = \lambda_{\min}(K_P) \text{tr}(Q^b \tilde{R}'\tilde{R}) \\ &\geq \lambda_{\min}(K_P) \lambda_{\min}(Q^b) \text{tr}(\tilde{R}'\tilde{R}) = \lambda_{\min}(K_P) \varepsilon \|\tilde{R}\|^2. \end{aligned}$$

(See [Kleinman and Athans \(1968\)](#) for the relevant trace inequality.) Using the property that $\text{tr}(\tilde{R}'RS(x)) = 0$ (due to symmetry of $\tilde{R}'\tilde{R}$; see, e.g., [Mahony et al. \(2008\)](#)), we can bound the first term on the right-hand side of Eq. (10) by $\sqrt{6}\|\tilde{R}\|\|\tilde{b}\|$. Similarly, we can bound the fourth term by $2\sqrt{3}\ell M_\omega \|\tilde{R}\|\|\tilde{b}\|$, where M_ω is a bound on $\|\omega^b\|$, and the fifth term by $2\sqrt{3}\ell(M_\omega + M_b) \|\tilde{R}\|\|\tilde{b}\|$. Using the additional properties that $\|\text{Proj}(\hat{b}, x)\| \leq \|x\|$ (see [Grip et al., 2012a](#), Lemma 3), $\|\text{vex}(\mathbb{P}_a(X))\| \leq \frac{1}{\sqrt{2}}\|X\|$, $\|\tilde{R}_s\| \leq 3$, and $\|J\| = \|\tilde{R}Q^b\| \leq M_Q \|\tilde{R}\|$, where $M_Q = qM_A^2$, we can bound the third term by $3\sqrt{3}\ell k_l \|K_P\| M_Q \|\tilde{R}\|^2$.

Considering next the sixth term on the right-hand side of Eq. (10), we have that $\text{tr}(S(\tilde{b})R'RS(\tilde{b})) = -\text{tr}(S'(\tilde{b})S(\tilde{b})) = -2\|\tilde{b}\|^2$, where we have used the property that $\text{tr}(S'(x)S(y)) = 2x'y$ (e.g., [Mahony et al., 2008](#)). For the eighth term, we have that

$$\begin{aligned} & -\tilde{b}' \text{Proj}(\hat{b}, -k_l \text{vex}(\mathbb{P}_a(\hat{R}_s' K_P J))) \leq k_l \tilde{b}' \text{vex}(\mathbb{P}_a(\hat{R}_s' K_P J)) \\ &= \frac{1}{2} k_l \text{tr}(S'(\tilde{b})\mathbb{P}_a(\hat{R}_s' K_P J)) = -\frac{1}{2} k_l \text{tr}(S(\tilde{b})\hat{R}_s' K_P J), \end{aligned}$$

where we have used the properties that $-\tilde{b}' \text{Proj}(\hat{b}, x) \leq -\tilde{b}'x$ (see [Grip et al., 2012a](#), Lemma 3) and $\text{tr}(S(x)X) = \text{tr}(S(x)\mathbb{P}_a(X))$ (e.g., [Mahony et al., 2008](#)). Considering the seventh and eighth term together, and using the fact that $\|R - \hat{R}_s\| \leq \|\tilde{R}\|$ we therefore have

$$\begin{aligned} & \ell\sigma \text{tr}(S(\tilde{b})R'K_P J) - 2\ell\sigma/k_l \tilde{b}' \text{Proj}(\hat{b}, -k_l \text{vex}(\mathbb{P}_a(\hat{R}_s' K_P J))) \\ &\leq \ell\sigma \text{tr}(S(\tilde{b})R'K_P J) - \ell\sigma \text{tr}(S(\tilde{b})\hat{R}_s' K_P J) \\ &\leq \sqrt{6}\ell\sigma \|K_P\| M_b M_Q \|\tilde{R}\|^2. \end{aligned}$$

Combining the inequalities, we can write

$$\begin{aligned} \dot{V} \leq & -\sigma \lambda_{\min}(K_P) \varepsilon \|\tilde{R}\|^2 + \sqrt{6}\|\tilde{R}\|\|\tilde{b}\| - 2\ell\|\tilde{b}\|^2 \\ & + 2\sqrt{3}\ell M_\omega \|\tilde{R}\|\|\tilde{b}\| + 2\sqrt{3}\ell(M_\omega + M_b) \|\tilde{R}\|\|\tilde{b}\| \\ & + 3\sqrt{3}\ell k_l \|K_P\| M_Q \|\tilde{R}\|^2 + \sqrt{6}\ell\sigma \|K_P\| M_b M_Q \|\tilde{R}\|^2 \\ = & -[\|\tilde{R}\| \quad \|\tilde{b}\|] \begin{bmatrix} \sigma\kappa_1 - \ell\kappa_2 - \ell\sigma\kappa_3 & -\kappa_4 - \ell\kappa_5 \\ -\kappa_4 - \ell\kappa_5 & 2\ell \end{bmatrix} \begin{bmatrix} \|\tilde{R}\| \\ \|\tilde{b}\| \end{bmatrix}, \end{aligned}$$

for positive constants $\kappa_1, \dots, \kappa_5$ that are independent of ℓ and σ . Let ℓ be small enough that $\kappa_1 - \ell\kappa_3 \geq \bar{\kappa}_1$ for some $\bar{\kappa}_1 > 0$. By investigating the resulting quadratic form, it is straightforward to show that \dot{V} can be made negative definite by choosing σ sufficiently large; hence, $\exists \alpha_3 > 0$ such that $\dot{V} \leq -\alpha_3(\|\tilde{R}\|^2 + \|\tilde{b}\|^2) \leq -\frac{\alpha_3}{\alpha_2} V$. By invoking the comparison lemma in the same way as in the exponential stability proof of [Khalil \(2002, Theorem 4.10\)](#), the result follows. ■

The result of [Lemma 1](#) guarantees stability of the error dynamics for all initial conditions that one would reasonably choose; the only restriction being that $\|\hat{b}(0)\| \leq M_{\hat{b}}$. In order to state a formal result of exponential stability from arbitrary initial conditions, we introduce the following resetting rule:

If at any time $t \geq 0$, $\|\hat{b}(t)\| > M_{\hat{b}}$, then \hat{b} is reset to

$$\hat{b}(t^+) = M_b \frac{\hat{b}(t)}{\|\hat{b}(t)\|}, \quad (11)$$

where t^+ denotes an infinitesimal time increment of t .

Theorem 1. Suppose that [Assumptions 1](#) and [2](#) hold and that A_j^b and A_j^n , $j \in 1, \dots, q$, have been designed to satisfy [Property 1](#). For any given choice of K_p and k_l , there exists a $\sigma^* \geq 1$ such that for all $\sigma \geq \sigma^*$, the origin of the error dynamics (8) is globally exponentially stable. \square

Proof. Considering the motion generated by the system from $t = 0$, if $\|\hat{b}(0)\| > M_{\hat{b}}$, then the state is immediately reset so that, on $(0, \infty)$ it behaves according to the Lipschitz continuous differential equations given in (8) with $\|\hat{b}\| \leq M_b$. From [Lemma 1](#) and the definition of global exponential stability in Section 1.2, the origin is therefore globally exponentially stable. \blacksquare

The requirements of [Theorem 1](#) can be met by choosing arbitrary gains K_p and k_l and gradually increasing σ until stability is achieved. In practice, K_p , k_l , and σ should be chosen through tuning; for example, by the use of simulations.

2.3. Estimates on SO(3)

A potential drawback of our approach is that the estimate \hat{R} is not guaranteed to belong to SO(3), even though it converges to SO(3). It is nevertheless possible to convert the estimates to SO(3), for example by the following algebraic formula:

$$\begin{aligned} \bar{R}(\hat{R}) &= [\bar{r}_1 \quad \bar{r}_2 \quad S(\bar{r}_1)\bar{r}_2], \\ \bar{r}_1 &= \hat{r}_1 / \max\{\|\hat{r}_1\|, \mu\}, \\ \bar{r}_2 &= (I_3 - \bar{r}_1\bar{r}_1')\hat{r}_2 / \max\{\|(I_3 - \bar{r}_1\bar{r}_1')\hat{r}_2\|, \mu\}, \end{aligned}$$

where \hat{r}_1 and \hat{r}_2 are the first and second columns of \hat{R} and $\mu \in (0, 1)$ is a small constant.

Proposition 1. The estimate $\bar{R}(\hat{R})$ is continuous in t on $(0, \infty)$ and $\lim_{t \rightarrow \infty} (R - \bar{R}(\hat{R})) = 0$. Furthermore, there exists a constant $T \geq 0$ such that for all $t \geq T$, $\bar{R}(\hat{R}) \in \text{SO}(3)$. \square

Proof. It is straightforward to verify that $\bar{R}(\hat{R})$ is a continuous function of \hat{R} (which is in turn continuous in t) and that $\bar{R}(R) = R$. Hence, since $\lim_{t \rightarrow \infty} \hat{R} = 0$, $\lim_{t \rightarrow \infty} (R - \bar{R}(\hat{R})) = 0$. Let $T > 0$ be large enough that for all $t \geq T$, $\|\hat{r}_1\| \geq \mu$ and $\|(I_3 - \bar{r}_1\bar{r}_1')\hat{r}_2\| \geq \mu$ (which is possible since both values converge to 1). Then for all $t \geq T$, \bar{r}_1 , \bar{r}_2 , and $\bar{r}_1 \times \bar{r}_2$ are orthonormal vectors. Since the third column of $\bar{R}(\hat{R})$ is the cross product of the first and the second, $\bar{R}(\hat{R}) \in \text{SO}(3)$. \blacksquare

The value $\bar{R}(\hat{R})$ represents a converging estimate of R that is guaranteed to belong to SO(3) after some initial transient. It is difficult to quantify the length of this transient, since it depends on the tuning of the observer and the choice of μ . As an example, we note that for the flight experiment presented in Section 4, one would obtain estimates on SO(3) for all $t \geq 0$ with any choice of μ less than 0.75.

2.4. Attitude estimation without [Assumption 1](#) and for single vector measurements

There may be situations where [Assumption 1](#) fails to hold, for example, due to sensor failure, magnetic disturbances, or particular maneuvers causing the vector measurements to be temporarily aligned. In the following, we show that the observer can still be used to estimate attitude if the vectors satisfy a certain PE condition. The results in this section assume that there is no gyro bias; if encountering a temporary situation in which [Assumption 1](#) fails to hold, one may in practice choose to apply the latest available bias estimate in order to minimize the error. We define the following alternative to [Property 1](#).

Property 2. For each $j \in 1, \dots, q$, the matrices A_j^n and A_j^b are piecewise continuous in t and uniformly bounded by $\|A_j^n\| = \|A_j^b\| \leq M_A$. Furthermore, they satisfy the relationship $A_j^n = RA_j^b$, and there exist constants $T > 0$ and $\bar{\varepsilon} > 0$ such that for all $t \geq 0$, $\int_t^{t+T} Q^n(\tau) d\tau \geq \bar{\varepsilon} I_3$, where Q^n is defined as before.

To analyze stability, suppose that $b = 0$ and consider the observer (2a) with $\hat{b} = 0$. The resulting error dynamics is

$$\dot{\tilde{R}} = \tilde{R}S(\omega^b) - \sigma K_p J. \quad (12)$$

Theorem 2. Suppose that A_j^b and A_j^n , $j \in 1, \dots, q$, have been designed to satisfy [Property 2](#). Then the origin of the error dynamics (12) is globally exponentially stable. \square

Proof. Consider the function $U = \frac{1}{2} \text{tr}(\tilde{R}'\tilde{R}(I_3 - \ell R'FR))$, where $F(t) = \int_t^\infty e^{t-\tau} Q^n(\tau) d\tau$ and $\ell > 0$ is yet to be determined. We have that $F = F' \geq 0$ and $\|F\| \leq M_Q$, and hence $U \leq \frac{1}{2} \|\tilde{R}\|^2$ and $U \geq \frac{1}{2} \|\tilde{R}\|^2(1 - \sqrt{3}\ell M_Q)$, which is positive definite for $\ell < 1/(\sqrt{3}M_Q)$. The derivative of U along the trajectories of (12) is given by

$$\begin{aligned} \dot{U} &= \frac{1}{2} \text{tr}(\tilde{R}'\dot{\tilde{R}}S(\omega^b)) - \frac{1}{2} \ell \text{tr}(\tilde{R}'\dot{\tilde{R}}S(\omega^b)R'FR) \\ &\quad - \frac{1}{2} \sigma \text{tr}(\tilde{R}'K_p J) + \frac{1}{2} \ell \sigma \text{tr}(\tilde{R}'K_p J R'FR) \\ &\quad - \frac{1}{2} \text{tr}(S(\omega^b)\tilde{R}'\dot{\tilde{R}}) + \frac{1}{2} \ell \text{tr}(S(\omega^b)\tilde{R}'\dot{\tilde{R}}R'FR) \\ &\quad - \frac{1}{2} \sigma \text{tr}(J'K_p \tilde{R}) + \frac{1}{2} \ell \sigma \text{tr}(J'K_p \tilde{R}R'FR) \\ &\quad + \frac{1}{2} \ell \text{tr}(\tilde{R}'\dot{\tilde{R}}S(\omega^b)R'FR) \\ &\quad - \frac{1}{2} \ell \text{tr}(\tilde{R}'\dot{\tilde{R}}R'FRS(\omega^b)) - \frac{1}{2} \ell \text{tr}(\tilde{R}'\dot{\tilde{R}}R'\dot{F}R). \end{aligned}$$

The first and the fifth term are zero due to the property $\text{tr}(XS(x)) = 0$ for symmetric X . The second and the ninth term cancel, as do the sixth and the tenth term, since $\text{tr}(\tilde{R}'\dot{\tilde{R}}R'FRS(\omega^b)) = \text{tr}(S(\omega^b)\tilde{R}'\dot{\tilde{R}}R'FR)$. Combining terms and using $J = \dot{\tilde{R}}Q^b$, $\dot{F} = F - Q^n$, and $Q^b = R'Q^nR$, we get

$$\begin{aligned} \dot{U} &= -\sigma \text{tr}(K_p \tilde{R}Q^b \tilde{R}') + \ell \sigma \text{tr}(\tilde{R}'K_p \tilde{R}Q^b R'FR) \\ &\quad - \frac{1}{2} \ell \text{tr}(\tilde{R}'\dot{\tilde{R}}R'FR) + \frac{1}{2} \ell \text{tr}(\tilde{R}'\dot{\tilde{R}}Q^b \tilde{R}') \\ &\leq -\sigma \lambda_{\min}(K_p) \|\tilde{R}\sqrt{Q^b}\|^2 + \frac{1}{2} \ell \|\tilde{R}\sqrt{Q^b}\|^2 \\ &\quad - \frac{1}{2} \ell \lambda_{\min}(R'FR) \|\tilde{R}\|^2 + \sqrt{3}\sigma \ell \|\tilde{R}\| \|K_p\| \|\tilde{R}\sqrt{Q^b}\| \bar{M}_Q M_Q, \end{aligned}$$

where \bar{M}_Q is a bound on $\sqrt{Q^b}$. We have

$$F \geq \int_t^{t+T} e^{t-\tau} Q^n(\tau) d\tau \geq e^{-T} \int_t^{t+T} Q^n(\tau) d\tau \geq e^{-T} \bar{\varepsilon} I_3.$$

Hence, $\lambda_{\min}(R'FR) = \lambda_{\min}(F) \geq e^{-T} \bar{\varepsilon}$. Consequently,

$$\dot{U} \leq - \left[\|\tilde{R}\sqrt{Q^b}\| \quad \|\tilde{R}\| \right] \begin{bmatrix} \kappa_1 - \ell\kappa_2 & -\ell\kappa_3 \\ -\ell\kappa_3 & \ell\kappa_4 \end{bmatrix} \begin{bmatrix} \|\tilde{R}\sqrt{Q^b}\| \\ \|\tilde{R}\| \end{bmatrix},$$

where $\kappa_1 = \sigma \lambda_{\min}(K_p)$, $\kappa_2 = \frac{1}{2}$, $\kappa_3 = \frac{1}{2} \sqrt{3} \sigma \bar{M}_Q M_Q \|K_p\|$, and $\kappa_4 = \frac{1}{2} e^{-T} \bar{\varepsilon}$. By investigating this quadratic form it is straightforward to show that \dot{U} is negative definite for all sufficiently small ℓ , and the result then follows from the comparison lemma (Khalil, 2002, Lemma 3.4). ■

In light of Theorem 2, let us consider the two alternative choices of A_j^b and A_j^n for $q = 1$ described by (6) and (7).

Proposition 2. Let A_1^n and A_1^b be chosen as described by either (6) or (7). If there exist constants $T > 0$ and $\bar{c}_{\text{obs}} > 0$ such that, for all $t \geq 0$, $\int_t^{t+T} \|w_1^n(\tau) \times w_2^n(\tau)\| d\tau \geq \bar{c}_{\text{obs}}$, then Property 2 is satisfied. □

A particular case for which Assumption 1 cannot hold is when only one pair of vector measurements, represented by w_1^b and w_1^n , is available. In this case we can apply the same injection terms with $w_2^b = w_2^n = 0$.

Proposition 3. Let A_1^n and A_1^b be chosen as $A_1^i = [w_1^i, 0, 0]$, for $i \in \{n, b\}$. If there exist constants $T > 0$ and $\bar{c}_{\text{obs}} > 0$ such that, for all $t \geq 0$, $\int_t^{t+T} w_1^n(\tau) w_1^n(\tau)' d\tau \geq \bar{c}_{\text{obs}} I_3$, then Property 2 is satisfied. □

The proofs of Propositions 2 and 3 are straightforward and omitted due to space constraints.

3. GNSS/INS integration

We now consider the design of a GNSS/INS integration observer, where position and linear velocity in the NED frame will be estimated together with the attitude and gyro bias. The system dynamics is given by

$$\dot{p}^n = v^n, \quad (13a)$$

$$\dot{v}^n = a^n + g^n, \quad (13b)$$

$$\dot{R} = RS(\omega^b), \quad (13c)$$

$$\dot{b} = 0, \quad (13d)$$

where p^n and v^n are the position and linear velocity, a^n is the proper acceleration, and g^n is the gravity vector. The sensor suite is assumed to consist of a GNSS receiver, 6-axis inertial instruments, and a 3-axis magnetometer (or another equivalent vector measurement). These instruments provide (i) a measurement of the NED position p^n ; (ii) a p -dimensional full or partial measurement of the NED linear velocity $v_m^n = C_v v^n$; (iii) a biased angular velocity measurement $\omega_m^b = \omega^b + b$, where b represents the bias; (iv) a linear accelerometer measurement a^b , which is related to a^n by $a^n = Ra^b$; and (v) a magnetometer measurement m^b , which is related to the Earth's magnetic field m^n at the current location by $m^n = Rm^b$.

We assume that the vectors a^n and m^n satisfy Assumption 1, and that the derivative \dot{a}^b of the accelerometer measurement is well-defined and bounded. We also assume that $\|a^b\|$ and $\|m^b\|$ are bounded by constants M_a and M_m .

3.1. Observer design

We shall make use of our observer from Section 2 to estimate R and b , and to do so we need two body-fixed vector measurements and corresponding reference vectors that satisfy Assumption 1. The vectors a^b , a^n , m^b , and m^n are natural candidates, and we therefore define matrices $A_j^b(a^b, m^b)$ and $A_j^n(a^n, m^n)$, $j \in 1, \dots, q$, to satisfy Property 1. We also require $A_j^n(a^n, m^n)$ to be everywhere locally Lipschitz continuous with respect to a^n , uniformly in t . We denote by $J(a^n, a^b, m^n, m^b, \hat{R})$ the injection term formed using $A_j^n(a^b, m^b)$ and $A_j^n(a^n, m^n)$ according to (3).

To deal with the fact that a^n is not directly measured, we observe that $a^n = Ra^b$ can be viewed as an input to the position and velocity dynamics (13a) and (13b), and leverage a design methodology for cascaded systems presented by Grip et al. (2012b). Following that methodology with some slight modifications, we introduce an estimate of a^n , denoted by \hat{a}^n . We furthermore define a saturated version of \hat{a}^n as $\hat{a}_s^n = \text{sat}_{M_a}(\hat{a}^n)$. We then implement the attitude and gyro bias observer with a^n replaced by \hat{a}_s^n :

$$\dot{\hat{R}} = \hat{R}S(\omega_m^b - \hat{b}) + \sigma K_p \hat{J}, \quad (14a)$$

$$\dot{\hat{b}} = \text{Proj}(\hat{b}, -k_l \text{vex}(\mathbb{P}_a(\hat{R}'_s K_p \hat{J}))), \quad (14b)$$

where $\hat{J} = J(\hat{a}_s^n, a^b, m^n, m^b, \hat{R})$. As before, any estimate \hat{b} such that $\|\hat{b}\| \geq M_b$ is reset as described in (11). The estimate \hat{a}^n is defined, together with estimates of p^n and v^n , as follows:

$$\dot{\hat{p}}^n = \hat{v}^n + K_{pp}(p^n - \hat{p}^n) + K_{pv}(v_m^n - C_v \hat{v}^n), \quad (15a)$$

$$\dot{\hat{v}}^n = \hat{a}^n + g^n + K_{vp}(p^n - \hat{p}^n) + K_{vv}(v_m^n - C_v \hat{v}^n), \quad (15b)$$

$$\dot{\xi} = -\sigma K_p \hat{J} a^b + K_{\xi p}(p^n - \hat{p}^n) + K_{\xi v}(v_m^n - C_v \hat{v}^n), \quad (15c)$$

$$\dot{\hat{a}}^n = \hat{R} a^b + \xi, \quad (15d)$$

where K_{pp} , K_{pv} , K_{vp} , K_{vv} , $K_{\xi p}$, and $K_{\xi v}$ are observer gains.

3.2. Stability

To analyze stability, we define the error variables $\tilde{p}^n = p^n - \hat{p}^n$ and $\tilde{v}^n = v^n - \hat{v}^n$. We then obtain the error dynamics

$$\dot{\tilde{p}}^n = \tilde{v}^n - K_{pp}\tilde{p}^n - K_{pv}C_v\tilde{v}^n, \quad (16a)$$

$$\dot{\tilde{v}}^n = \tilde{a}^n - K_{vp}\tilde{p}^n - K_{vv}C_v\tilde{v}^n, \quad (16b)$$

where $\tilde{a}^n = a^n - \hat{a}^n$. By differentiating \tilde{a}^n , we find that

$$\dot{\tilde{a}}^n = -K_{\xi p}\tilde{p}^n - K_{\xi v}C_v\tilde{v}^n + \tilde{d}, \quad (17)$$

where $\tilde{d} = (RS(\omega^b) - \hat{R}S(\omega_m^b - \hat{b}))a^b + (R - \hat{R})\dot{a}^b$. Defining $\tilde{x} = [\tilde{p}^n; \tilde{v}^n; \tilde{a}^n]$, we can write (16), (17) more compactly as

$$\dot{\tilde{x}} = (A - KC)\tilde{x} + B\tilde{d}, \quad (18)$$

$$A = \begin{bmatrix} 0 & I_6 \\ 0 & 0 \end{bmatrix}, \quad B = \begin{bmatrix} 0 \\ I_3 \end{bmatrix}, \quad C = \begin{bmatrix} I_3 & 0 & 0 \\ 0 & C_v & 0 \end{bmatrix},$$

$$K = \begin{bmatrix} K_{pp} & K_{pv} \\ K_{vp} & K_{vv} \\ K_{\xi p} & K_{\xi v} \end{bmatrix}.$$

The dynamics of the errors \tilde{R} and \tilde{b} becomes the same as in (8), but with J replaced by \hat{J} :

$$\dot{\tilde{R}} = RS(\omega^b) - \hat{R}S(\omega_m^b - \hat{b}) - \sigma K_p \hat{J}, \quad (19a)$$

$$\dot{\tilde{b}} = -\text{Proj}(\hat{b}, -k_l \text{vex}(\mathbb{P}_a(\hat{R}'_s K_p \hat{J}))). \quad (19b)$$

Theorem 3. Suppose that *Assumptions 1* and *2* hold and that $A_j^b(a^b, m^b)$ and $A_j^n(a^n, m^n)$ have been designed to satisfy *Property 1*. Let σ be chosen to ensure stability according to *Theorem 1* and define $H_K(s) := (Is - A + KC)^{-1}B$. There exists a $\gamma > 0$ such that, if the gain matrix K is chosen such that $A - KC$ is Hurwitz and $\|H_K(s)\|_\infty < \gamma$, then the origin of the error dynamics (18), (19) is globally exponentially stable. Moreover, K can always be chosen to satisfy these conditions. \square

Proof. Because (A, C) is observable and (A, B, C) is left-invertible and minimum-phase, K can be chosen to satisfy the requirements of *Theorem 3* (see Grip et al., 2012b, proof of Theorem 2). If $\|\hat{b}(0)\| > M_{\hat{b}}$, then the bias estimate is immediately reset, and the parameter projection ensures that the solutions cannot escape the region defined by $\|\hat{b}\| \leq M_{\hat{b}}$.

The error dynamics (19) can be written as

$$\dot{\tilde{R}} = R S(\omega^b) - \hat{R} S(\omega_m^b - \hat{b}) - \sigma K_P J + \sigma K_P \tilde{J},$$

$$\dot{\tilde{b}} = -\text{Proj}(\hat{b}, \beta(J)) + \text{Proj}(\hat{b}, \beta(J)) - \text{Proj}(\hat{b}, \beta(\hat{J})),$$

where $\tilde{J} = J - \hat{J}$ and $\beta(J) = -k_l \text{vex}(\mathbb{P}_a(\hat{R}'_s K_P J))$. We can write $\tilde{J} = \sum_{j=1}^q (A_j^n(a^n, m^n) - A_j^n(\hat{a}_s^n, m^n)) A_j^b(a^b, m^b)'$, and it follows that $\|\tilde{J}\| \leq M_A \sum_{j=1}^q \|A_j^n(a^n, m^n) - A_j^n(\hat{a}_s^n, m^n)\|$. Since $A_j^n(a^n, m^n)$ is locally Lipschitz, uniformly in t , with respect to a^n , and since a^n and \hat{a}_s^n are bounded, there is a $\kappa_1 > 0$ such that $\|A_j^n(a^n, m^n) - A_j^n(\hat{a}_s^n, m^n)\| \leq \frac{\kappa_1}{M_A q} \|a^n - \hat{a}_s^n\| \leq \frac{\kappa_1}{M_A q} \|\tilde{a}^n\|$. Hence $\|\sigma K_P \tilde{J}\| \leq \sigma \|K_P\| \kappa_1 \|\tilde{a}^n\|$. Using the techniques of the proof of *Lemma 1*, we can easily show that there is a $\kappa_2 > 0$ such that $\|\beta(J) - \beta(\hat{J})\| \leq \kappa_2 \|\tilde{a}^n\|$. It can therefore be verified that there exists a $\kappa_3 > 0$ such that $\|\text{Proj}(\hat{b}, \beta(J)) - \text{Proj}(\hat{b}, \beta(\hat{J}))\| \leq \kappa_3 \|\tilde{a}^n\|$.

Considering V from the proof of *Lemma 1*, we have that

$$\begin{aligned} \dot{V} &\leq -\alpha_3 (\|\tilde{R}\|^2 + \|\tilde{b}\|^2) - \ell \text{tr}(S(\tilde{b}) R' \sigma K_P \tilde{J}) \\ &\quad - \ell \text{tr}(S(\text{Proj}(\hat{b}, \beta(J)) - \text{Proj}(\hat{b}, \beta(\hat{J}))) R' \tilde{R}) \\ &\quad + \text{tr}(\tilde{R}' \sigma K_P \tilde{J}) + \frac{2\sigma\ell}{k_l} \tilde{b}' (\text{Proj}(\hat{b}, \beta(J)) - \text{Proj}(\hat{b}, \beta(\hat{J}))) \\ &\leq -\alpha_3 (\|\tilde{R}\|^2 + \|\tilde{b}\|^2) + \frac{2\sigma\ell\kappa_3}{k_l} \|\tilde{b}\| \|\tilde{a}^n\| + \sqrt{6}\ell\kappa_3 \|\tilde{R}\| \|\tilde{a}^n\| \\ &\quad + \sqrt{6}\ell\sigma \|K_P\| \kappa_1 \|\tilde{b}\| \|\tilde{a}^n\| + \sqrt{3}\sigma \|K_P\| \kappa_1 \|\tilde{R}\| \|\tilde{a}^n\| \\ &\leq -\alpha_3 \zeta^2 + \kappa_4 \zeta \|\tilde{x}\| \end{aligned}$$

for some $\kappa_4 > 0$, where $\zeta := (\|\tilde{R}\|^2 + \|\tilde{b}\|^2)^{1/2}$. Following the proof of Grip et al. (2012b, Theorem 1), there is a positive-definite function $W = \tilde{x}' P \tilde{x}$ such that $\dot{W} \leq -\|\tilde{x}\|^2 + \gamma^2 \|\tilde{d}\|^2$. We can rewrite \tilde{d} as $(\tilde{R} S(\omega^b) - \tilde{R} S(\hat{b}) + \tilde{R} S(\hat{b})) a^b + \tilde{R} \hat{a}^b$, which is bounded by $\sqrt{2}(M_\omega M_a \|\tilde{R}\| + M_a \|\tilde{b}\| + M_{\hat{b}} M_a \|\tilde{R}\|) + M_{\hat{a}} \|\tilde{R}\|$, where $M_{\hat{a}}$ is a bound on \hat{a}^b . Hence, $\dot{W} \leq -\|\tilde{x}\|^2 + \gamma^2 \kappa_5^2 \zeta^2$ for some $\kappa_5 > 0$. Defining $Y = W + \gamma V$ and computing \dot{Y} , we obtain a quadratic form in $\|\tilde{x}\|$ and ζ , which is negative definite for all sufficiently small γ . The result now follows from the comparison lemma (Khalil, 2002, Lemma 3.4). \blacksquare

Stability for the GNSS/INS integration observer can also be proven under the relaxed PE condition from *Theorem 2*, albeit without gyro bias estimation. We omit the proof of this statement due to space constraints.

4. Validation using experimental flight data

In this section we test the GNSS/INS integration algorithm using data from an xsens MTI IMU and a u-Blox LEA-6H GNSS receiver, mounted in a Piper Cherokee 140 light fixed-wing aircraft. The IMU includes a magnetometer and provides data at 100 Hz, while

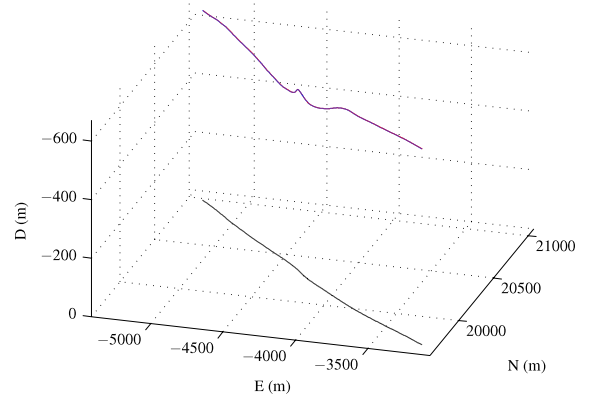


Fig. 1. The measured (blue) and estimated (red) positions (ground track at zero altitude in black) for stall maneuver.

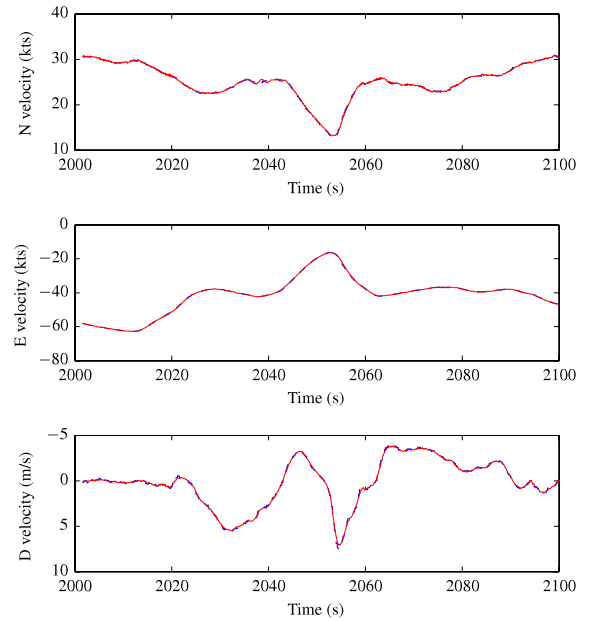


Fig. 2. The measured (blue, dashed) and estimated (red, solid) velocities for stall maneuver. (For interpretation of the references to color in this figure legend, the reader is referred to the web version of this article.)

the GNSS receiver provides position and Doppler-based velocity measurements at 5 Hz.

The observer is implemented using forward-Euler discretization at 100 Hz. All measurements are filtered using a 5 Hz, second-order low-pass filter. We implement the attitude observer using an injection term with $q = 2$, where A_1^n and A_1^b are defined according to (6) with vectors $\hat{a}_s^n/5$ and $a^b/5$, $m^n/\|m^n\|$, and $m^b/\|m^b\|$; and A_2^n and A_2^b are defined in the same way with the order of the vectors reversed. The gains chosen for the attitude observer are $K_p = I_3$, $\sigma = 1$, and $k_l = 0.01$. With the help of an LMI formulation that allows $\|H_K(s)\|_\infty$ to be reduced as necessary, we choose $K_{pp} \approx 3.3I_3$, $K_{pv} \approx 2.74I_3$, $K_{vp} \approx 0.03I_3$, $K_{vv} \approx 2.36I_3$, $K_{\xi p} \approx 0.01I_3$, and $K_{\xi v} \approx 1.07I_3$, for which $\|H_K(s)\|_\infty \approx 2.5$.

To provide a reference for the attitude we smooth all the measurements using a non-causal zero-phase filter with a 1 Hz cutoff frequency and differentiate the filtered velocity measurement numerically to obtain a^n . One reference is then generated by computing the algebraic QUEST solution (see Shuster & Oh, 1981), and a second reference is generated using a multiplicative extended Kalman filter (MEKF) (Markley, 2003). A separate reference for the

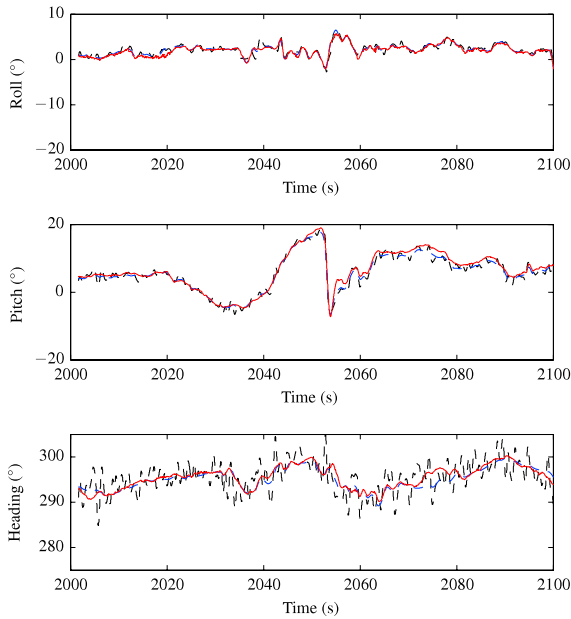


Fig. 3. QUEST (black, dashed), MEKF (blue, dashed), and observer (red, solid) attitude estimates for stall maneuver.

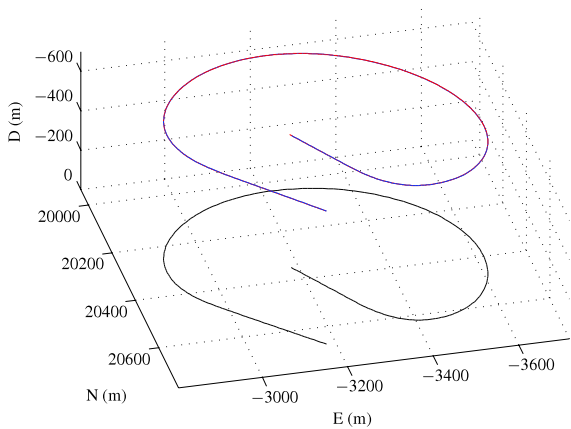


Fig. 4. The measured (blue) and estimated (red) positions (ground track at zero altitude in black) for steep turn maneuver.

gyro bias is computed by averaging the gyro measurements at standstill before and after the flight.

Since we do not have an independent, authoritative reference for the attitude and gyro bias, the results displayed here are not intended as a performance evaluation or a comparison of different methodologies; rather, they are intended as a proof of concept and verification of the theoretical stability results.

4.1. Maneuvers

We present results for three different maneuvers. The first maneuver is an approach stall with recovery. The position estimate for this maneuver is compared with the measured GNSS position in Fig. 1, with the ground track at zero altitude shown below. The velocity estimate is compared with the measured GNSS velocity in Fig. 2. In Fig. 3, the attitude estimate is compared to the QUEST and MEKF solutions. The attitude is displayed in Euler angles, which for the observer were computed from the elements of \hat{R} (see, e.g., Fos- sen, 2011). The second maneuver is a 360° steep turn at approximately 45° bank angle. The results of this maneuver are displayed in Figs. 4–6. The third maneuver is a left-handed traffic pattern flown from takeoff to landing, with results displayed in Figs. 7–9.

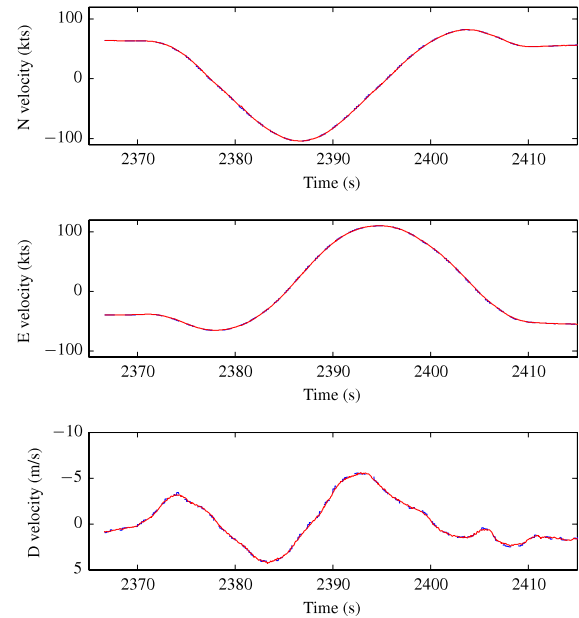


Fig. 5. The measured (blue, dashed) and estimated (red, solid) velocities for steep turn maneuver. (For interpretation of the references to color in this figure legend, the reader is referred to the web version of this article.)

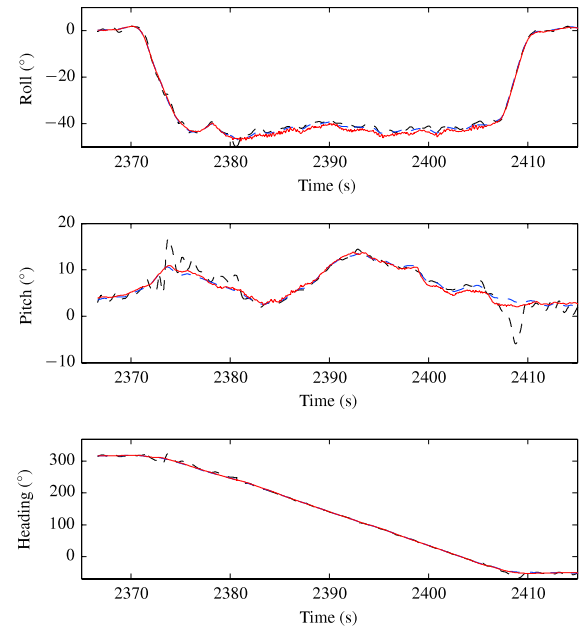


Fig. 6. QUEST (black, dashed), MEKF (blue, dashed), and observer (red, solid) attitude estimates for steep turn maneuver.

Despite some discrepancies between the attitude estimate and the references, there is no question about the generally high level of agreement. The benefits of integrating vector and gyro measurements can be observed from the sometimes erratic behavior of the QUEST solution, despite the heavy filtering of the vectors used to produce it. In Fig. 10 we show the estimated gyro bias for the entire flight, together with the bias estimate from the MEKF and the reference computed at standstill. The choice of k_I in the observer (and, similarly, the tuning of the MEKF) means that the bias estimate changes quite rapidly; a smaller k_I would result in a more

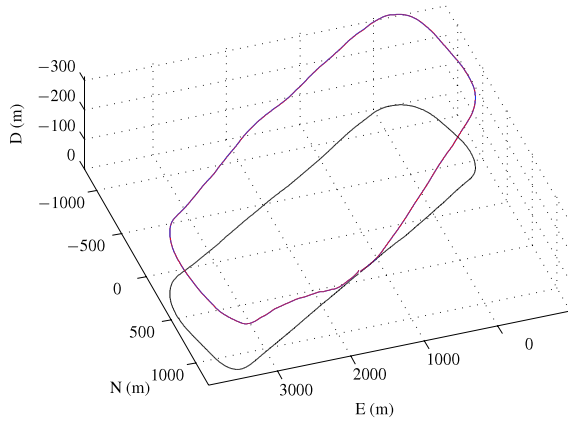


Fig. 7. The measured (blue) and estimated (red) positions (ground track at zero altitude in black) for traffic pattern maneuver.

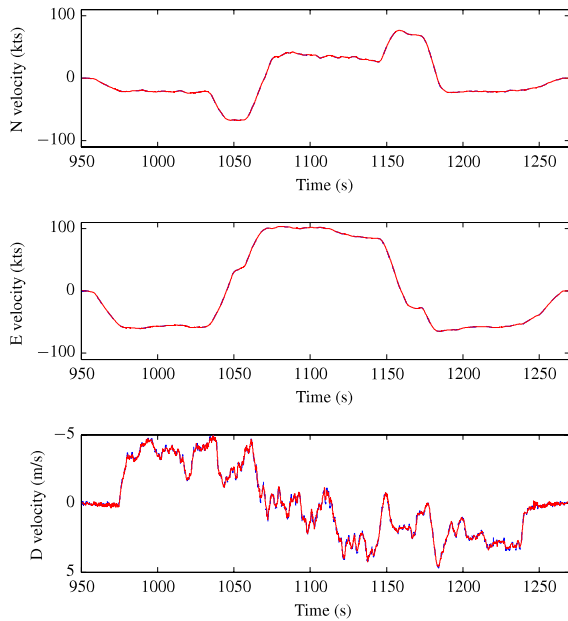


Fig. 8. The measured (blue, dashed) and estimated (red, solid) velocities for traffic pattern maneuver. (For interpretation of the references to color in this figure legend, the reader is referred to the web version of this article.)

slowly-varying estimate. The relationship between the bias estimate and the references is nevertheless evident.

5. Concluding remarks

In this paper we have introduced an observer that provides globally exponentially stable estimates of attitude and gyro bias based on a set of body-fixed vector measurements and corresponding reference vectors, which are allowed to be time-varying. We have furthermore used the attitude observer as part of a complete GNSS/INS integration design. The validity of the design and analysis is confirmed by flight tests, although little can be said about performance at this point. A proper test of performance, with independent references and a comparison with other algorithms, is a topic of future research.

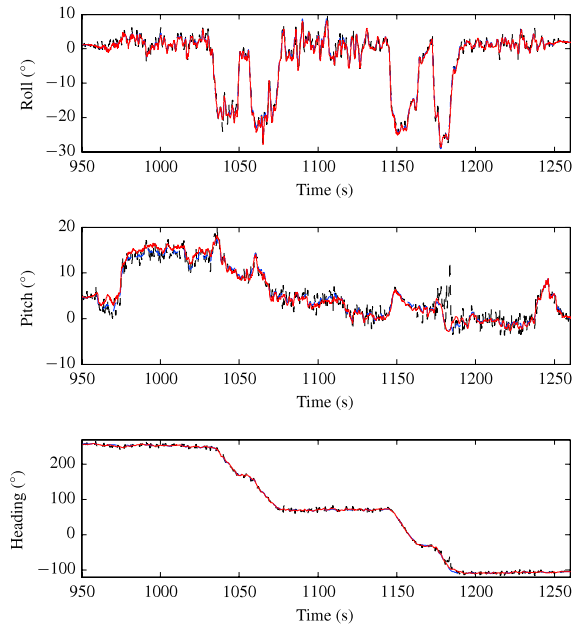


Fig. 9. QUEST (black, dashed), MEKF (blue, dashed), and observer (red, solid) attitude estimates for traffic pattern maneuver.

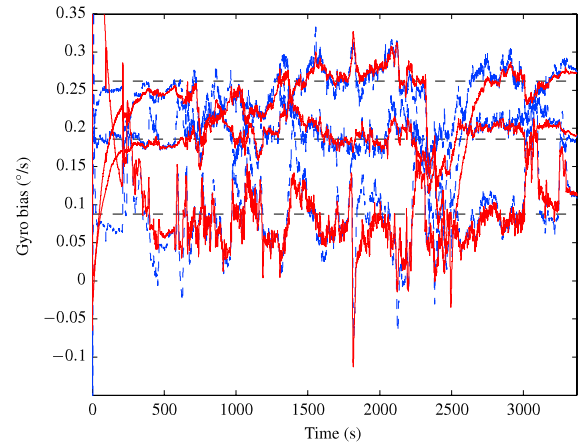


Fig. 10. Gyro bias computed at standstill (black, dashed), estimate from MEKF (blue, dashed), and estimate from observer (red, solid).

Appendix. Projection

The parameter projection $\text{Proj}(\cdot, \cdot)$ used for the gyro bias estimation is defined as

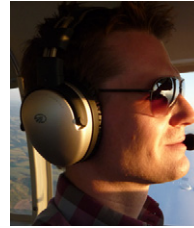
$$\text{Proj}(\hat{b}, \beta) = \begin{cases} \left(I_3 - \frac{c(\hat{b})}{\|\hat{b}\|^2} \hat{b} \hat{b}' \right) \beta, & \|\hat{b}\| \geq M_b, \quad \hat{b}' \beta > 0, \\ \beta, & \text{otherwise,} \end{cases}$$

where $c(\hat{b}) = \min\{1, (\|\hat{b}\|^2 - M_b^2)/(M_b^2 - M_b^2)\}$. This is a special case of the parameter projection from Krstić, Kanellakopoulos, and Kokotović (1995, App. E).

References

- Batista, P., Silvestre, C., & Oliveira, P. J. (2011a). GES attitude observers – Part I: Multiple general vector observations. In *Proc. IFAC World Congr.* Milan, Italy (pp. 2985–2990).
- Batista, P., Silvestre, C., & Oliveira, P. J. (2011b). GES attitude observers – Part II: Single vector observations. In *Proc. IFAC world congr.* Milan, Italy (pp. 2991–2996).

- Batista, P., Silvestre, C., & Oliveira, P. (2012a). A GES attitude observer with single vector observations. *Automatica*, 48(2), 388–395.
- Batista, P., Silvestre, C., & Oliveira, P. (2012b). Globally exponentially stable cascade observers for attitude estimation. *Control Engineering Practice*, 20, 148–155.
- Batista, P., Silvestre, C., & Oliveira, P. (2012c). Sensor-based globally asymptotically stable filters for attitude estimation: Analysis, design, and performance evaluation. *IEEE Transactions on Automatic Control*, 57(8), 2095–2100.
- Bhat, S. P., & Bernstein, D. S. (2000). A topological obstruction to continuous global stabilization of rotational motion and the unwinding phenomenon. *Systems & Control Letters*, 39, 63–70.
- Crassidis, J. L., Markley, F. L., & Cheng, Y. (2007). Survey of nonlinear attitude estimation methods. *Journal of Guidance Control and Dynamics*, 30(1), 12–28.
- Fossen, T. I. (2011). *Handbook of marine craft hydrodynamics and motion control*. Wiley.
- Grip, H. F., Fossen, T. I., Johansen, T. A., & Saberi, A. (2012a). A nonlinear observer for integration of GNSS and IMU measurements with gyro bias estimation. In *Proc. American contr. conf. Montreal, Canada*, (pp. 4607–4612).
- Grip, H. F., Saberi, A., & Johansen, T. A. (2011). Observers for cascaded nonlinear and linear systems. In *Proc. IEEE conf. dec. contr. Orlando, FL*, (pp. 3331–3337).
- Grip, H. F., Saberi, A., & Johansen, T. A. (2012b). Observers for interconnected nonlinear and linear systems. *Automatica*, 48(7), 1339–1346.
- Hamel, T., & Mahony, R. (2006). Attitude estimation on SO(3) based on direct inertial measurements. In *Proc. IEEE int. conf. robotics automation. Orlando, FL*, (pp. 2170–2175).
- Hua, M.-D. (2010). Attitude estimation for accelerated vehicles using GPS/INS measurements. *Control Engineering Practice*, 18(7), 723–732.
- Khalil, H. K. (2002). *Nonlinear systems* (3rd ed.). Upper Saddle River, NJ: Prentice-Hall.
- Kinsey, J., & Whitcomb, L. L. (2007). Adaptive identification on the group of rigid-body rotations and its application to underwater vehicle navigation. *IEEE Transactions on Robotics*, 23(1), 124–136.
- Kleinman, D. L., & Athans, M. (1968). The design of suboptimal linear time-varying systems. *IEEE Transactions on Automatic Control*, 13, 150–159.
- Krstić, M., Kanellakopoulos, I., & Kokotović, P. V. (1995). *Nonlinear and adaptive control design*. New York: Wiley.
- Lee, T., Leok, M., McClamroch, N., & Sanyal, A. (2007). Global attitude estimation using single direction measurements. In *Proc. American contr. conf. New York City, NY*, (pp. 3659–3664).
- Lefferts, E. J., Markley, F. L., & Shuster, M. D. (1982). Kalman filtering for spacecraft attitude estimation. In *Proc. AIAA 20th aerospace sciences meeting* (pp. 1–16).
- Mahony, R., Hamel, T., & Pflimlin, J.-M. (2008). Nonlinear complementary filters on the Special Orthogonal Group. *IEEE Transactions on Automatic Control*, 53(5), 1203–1218.
- Mahony, R., Hamel, T., Trumpf, J., & Lageman, C. (2009). Nonlinear observers on SO(3) for complementary and compatible measurements: A theoretical study. In *Proc. IEEE conf. dec. contr. Shanghai, China*, (pp. 6407–6412).
- Markley, F. L. (2003). Attitude error representations for Kalman filtering. *J. Guid. Contr. Dynam.*, 26(2), 311–317.
- Maybeck, P. S. (1979). Stochastic models, estimation, and control, volume 1. In *Mathematics in science and engineering: Vol. 141*. New York: Academic Press.
- Michel, A., Hou, L., & Liu, D. (2008). *Stability of dynamical systems: continuous, discontinuous, and discrete systems*. Birkhäuser.
- Phillips, R., & Schmidt, G. (1996). GPS/INS integration. In *AGARD lecture series: system implications and innovative applications of satellite navigation: Vol. 207* (pp. 9.1–9.18).
- Salcudean, S. (1991). A globally convergent angular velocity observer for rigid body motion. *IEEE Transactions on Automatic Control*, 36(12), 1493–1497.
- Shuster, M. D., & Oh, S. D. (1981). Three-axis attitude determination from vector observations. *J. Guid. Contr. Dynam.*, 4(1), 70–77.
- Thienel, J. K., & Sanner, R. M. (2003). A coupled nonlinear spacecraft attitude controller and observer with an unknown constant gyro bias and gyro noise. *IEEE Transactions on Automatic Control*, 48(11), 2011–2015.
- Vasconcelos, J. F., Silvestre, C., & Oliveira, P. (2008). A nonlinear observer for rigid body attitude estimation using vector observations. In *Proc. IFAC world congr. Seoul, South Korea*, (pp. 8599–8604).
- Vik, B., & Fossen, T. I. (2001). A nonlinear observer for GPS and INS integration. In *Proc. IEEE conf. dec. contr. Orlando, FL*, (pp. 2956–2961).



Håvard Fjær Grip graduated from the Department of Engineering Cybernetics at the Norwegian University of Science and Technology (NTNU) with an M.Sc. in 2006 and a Ph.D. in 2010. He has worked as a scientific researcher for SINTEF ICT, Applied Cybernetics, on automotive estimation problems, including a contract project in 2007–2008 with Daimler Group Research and Advanced Engineering in Stuttgart, Germany. He conducted an independent research project at Washington State University (WSU) in Pullman, Washington, from 2010 to 2012, funded by the Research Council of Norway. He currently works as a research technologist at NASA's Jet Propulsion Laboratory in Pasadena, California. He also holds an Adjunct Associate Professorship at NTNU and an Adjunct Assistant Professorship at WSU.



Thor I. Fossen was born in 1963 and he received the M.Sc. degree in Naval Architecture and the Ph.D. in Engineering Cybernetics in 1987 and 1991, both from the Norwegian University of Science and Technology (NTNU). In the period 1989–1990 he pursued postgraduate studies as a Fulbright Scholar in aerodynamics and flight control at the Department of Aeronautics and Astronautics, University of Washington, Seattle. In 1993 Fossen was appointed as a Professor of Guidance, Navigation and Control at NTNU and he was elected into the Norwegian Academy of Technological Sciences in 1998. Fossen is currently the co-director of the CoE Centre for Autonomous Marine Operations and Systems (AMOS). Fossen is teaching mathematical modeling of aircraft, marine craft, unmanned vehicles and nonlinear control theory. Fossen has authored approximately 300 scientific papers and 5 textbooks including the Wiley textbooks *Guidance and Control of Ocean Vehicles* and *Handbook of Marine Craft Hydrodynamics and Motion Control*. He has served as Associate Editor of *Automatica*. Fossen is one of the co-founders of Marine Cybernetics where he was Vice President of R&D in the period 2002–2008. A patent for weather optimal positioning control of marine vessels was granted in 1998. This work received the Automatica Prize Paper Award in 2002. In 2008 he received the Arch T. Colwell Merit Award at the SAE 2008 World Congress for a paper entitled Nonlinear Observer for Vehicle Velocity Estimation.



Tor A. Johansen (M.Sc., Ph.D.) worked at SINTEF Electronics and Cybernetics as a researcher before he was appointed Associate Professor at the Norwegian University of Science and Technology in Trondheim in 1997 and was promoted to Professor in 2001. He has published more than 100 articles in international journals as well as numerous conference articles and book chapters in the areas of control, estimation and optimization with applications in the marine, automotive, biomedical and process industries. In 2002 Johansen co-founded the company Marine Cybernetics AS where he was Vice President until 2008.

Prof. Johansen is currently a principal researcher within the Center of Excellence on Autonomous Marine Operations and Systems (AMOS) and director of the UAV Laboratory at NTNU.

Ali Saberi lives and works in Pullman, Washington.